



**Abstract**—Many rockfishes (*Sebastes* spp.) inhabit rugged areas of seafloor that are inaccessible to survey trawl gear. Their utilization of such habitat makes estimation of their abundance difficult. Furthermore, it is often difficult to assess whether habitat is trawlable or untrawlable and to estimate the spatial extent of both habitat types. To help determine trawlability for the continental shelf in the Gulf of Alaska, we used multibeam sonar data collected in the area during 2011, 2013, and 2015. These data were used to derive 3 characteristics of the seafloor: oblique incidence backscatter strength ( $S_b$ , oblique), seafloor ruggedness, and bathymetric position index. Habitat type was categorized as trawlable or untrawlable through analysis of video from deployed drift cameras. We tested the effectiveness of the use of these seafloor characteristics in prediction of habitat trawlability with 4 types of models: generalized linear model, generalized additive model, boosted regression tree, and random forest. All 4 models perform moderately well at predicting trawlability across the shelf, and results from all of them indicate that  $S_b$ , oblique is the most important characteristic in discriminating between trawlable and untrawlable habitat. These results indicate that multibeam sonar data can help determine habitat type, information that in turn can help improve habitat-specific estimates of biomass of marine fish species.

Manuscript submitted 11 September 2020.  
Manuscript accepted 18 August 2021.  
Fish. Bull. 119:184–196 (2021).  
Online publication date: 13 September 2021.  
doi: [10.7755/FB.119.2-3.7](https://doi.org/10.7755/FB.119.2-3.7)

The views and opinions expressed or implied in this article are those of the author (or authors) and do not necessarily reflect the position of the National Marine Fisheries Service, NOAA.

## Comparison of model types for prediction of seafloor trawlability in the Gulf of Alaska by using multibeam sonar data

Sarah C. Stienessen (contact author)<sup>1</sup>

Christopher N. Rooper<sup>2</sup>

Thomas C. Weber<sup>3</sup>

Darin T. Jones<sup>1</sup>

Jodi L. Pirtle<sup>4</sup>

Christopher D. Wilson<sup>1</sup>

Email address for contact author: [sarah.stienessen@noaa.gov](mailto:sarah.stienessen@noaa.gov)

<sup>1</sup> Alaska Fisheries Science Center  
National Marine Fisheries Service, NOAA  
7600 Sand Point Way NE  
Seattle, Washington 98115

<sup>2</sup> Stock Assessment and Research Division  
Pacific Biological Station  
Fisheries and Oceans Canada  
3190 Hammond Bay Road  
Nanaimo, V9T 6N7 Canada

<sup>3</sup> Center for Coastal and Ocean Mapping  
University of New Hampshire  
24 Colovos Road  
Durham, New Hampshire 03824

<sup>4</sup> Alaska Regional Office  
National Marine Fisheries Service, NOAA  
P.O. Box 21668  
Juneau, Alaska 99802

The bottom-trawl surveys conducted by the Alaska Fisheries Science Center (AFSC) provide estimates of biomass of numerous rockfishes (*Sebastes* spp.) in the Gulf of Alaska (GOA) (Aydin et al., 2019). An area-swept method is used for the bottom-trawl surveys conducted over trawlable areas within the GOA (von Szalay and Raring, 2018). Results (e.g., biomass and numbers of various fish species) obtained from surveys in trawlable areas are expanded to the entire GOA, including untrawlable areas (i.e., those locations where the structure of the seafloor prevents survey gear from being properly or successfully deployed according to survey protocols). The biomass estimates from bottom-trawl surveys are essential input for stock assessment efforts and data-based fisheries management. However, many rockfish species prefer rocky and rugged habitat that is often inaccessible to bottom-trawl gear; in other words, many rockfish

species reside at higher densities in untrawlable habitats (Jagiello et al., 2003). Acoustic backscatter attributed to individual rockfish in untrawlable areas is estimated to be 3 times that of backscatter attributed to individuals in trawlable areas (Jones et al., 2021).

By not sampling the preferred (untrawlable) habitat of some rockfish species, the biomass of these species in the GOA can be underestimated. Similarly, by sampling only the preferred (trawlable) habitat for other rockfish species, the biomass of these species can be overestimated. Survey efforts targeting only one of the habitat types occupied by a species can add non-random error to biomass estimates (Cordue, 2007). Consequently, reliable assessments of rockfish species are needed for both trawlable and untrawlable habitat types in the surveyed area. Acoustic methods, with complementary direct sampling tools, are being used to assess semi-pelagic

rockfish populations that cannot be successfully sampled with trawl nets (Williams et al., 2010; Jones et al., 2012; Rooper et al., 2012; Jones et al., 2021).

During the AFSC bottom-trawl surveys, trawl tows are conducted at stations selected by using a stratified random sampling design (von Szalay and Raring, 2018). Historically, 25-km<sup>2</sup> grid cells have been designated as either trawlable or untrawlable; however, the initial classification of a grid cell is often uncertain. The trawlability of the seafloor in grid cells has been determined by a vessel skipper searching for a minimum of 2 h to locate trawlable ground with a multibeam echo sounder. Realistically, knowledge of seafloor trawlability is not complete across each grid cell, and most grid cells include both trawlable and untrawlable bottom types. For an entire grid cell to be designated as trawlable, a trawlable path of only 1.5 km along the seafloor is necessary (1.5 km is the trawl length of a standard 15-min bottom-trawl tow). Trawling in an untrawlable area within a grid cell classified as trawlable can result in substantial gear damage, lost survey time, habitat damage, and the cell may end up being reclassified as untrawlable. More accurate knowledge of the actual extent of trawlable and untrawlable areas within the grid cells of a bottom-trawl survey can help to improve biomass estimates and survey productivity.

Research efforts have used the combination of acoustic backscatter data and analysis of underwater camera video to improve estimates of availability of rockfish species in the GOA, in part by using video images to determine the extent of seafloor trawlability (e.g., Jones et al., 2012; Rooper et al., 2012; Jones et al., 2021). These studies are limited by the time it takes to deploy a camera and the area that can be covered by a single camera. Multibeam sonar systems collect high-resolution acoustic bathymetry and backscatter data. These data can be used to generate comprehensive images of the seafloor, describe features of seafloor morphology, and discriminate among substrate types (e.g., Jagielo et al., 2003; Goff et al., 2004; Wilson et al., 2007; Brown and Blondel, 2009; Weber et al., 2013). If multibeam sonar data can be used to successfully categorize seafloor trawlability, large areas of seafloor can be classified as trawlable or untrawlable quickly and efficiently.

Researchers with the AFSC and the Center for Coastal and Ocean Mapping at the University of New Hampshire began collaborating in 2008 to optimize standard operating procedures for seafloor mapping with a Simrad ME70<sup>1</sup> multibeam echo sounder (Kongsberg Maritime AS, Kongsberg, Norway). The Simrad ME70 was designed specifically for fishery research applications as a calibrated, user-configurable multibeam sonar system intended to collect quantitative data on acoustic targets in the water column (Trenkel et al., 2008; Stienessen et al., 2019). However, the Simrad ME70 can also be used to simultaneously collect bathymetry and seafloor backscatter data (Cutter

et al., 2010). Customized software can be used to extract bottom detections that characterize the seafloor from data collected with a Simrad ME70 (Weber et al., 2013).

A case study at Snakehead Bank, off Kodiak Island in Alaska, used seafloor characteristics extracted from the multibeam data collected with a Simrad ME70 in tandem with analysis of video images to distinguish trawlable from untrawlable habitat in the GOA (Weber et al., 2013). In a subsequent study, more areas in the GOA were included, several characteristics of benthic terrain derived from multibeam sonar data at various scales were considered, and optical technology was used to validate seafloor classification derived from multibeam sonar data (Pirtle et al., 2015). The authors of the latter study reported that the 2 best generalized linear models (GLMs) described 54% of the variation between trawlable and untrawlable seafloor types. These quantitative models were developed by using data collected with a Simrad ME70, at stations where video data were also recorded, and combined either oblique incidence backscatter strength ( $S_b$ , oblique) or mosaic seafloor backscatter strength with vector ruggedness measure (VRM) and bathymetric position index (BPI) to predict seafloor trawlability.

Each of the predictors identified by Pirtle et al. (2015) describe a component of seafloor morphology. Backscatter strength is dependent on incidence angle of the acoustic signal with the seafloor. At normal incidence, there is not much difference in  $S_b$  between strong scatterers (e.g., hard rock and boulders) and weak ones (e.g., fine sand). However,  $S_b$  is higher from strong scatterers than from weak scatterers when the incidence angle is oblique (Jackson and Richardson, 2007; Lamarche et al., 2011; Weber et al., 2013). Values of  $S_b$  oblique can therefore help differentiate between substrate types. Vector ruggedness measure is a measure of seafloor rugosity (i.e., seafloor complexity), and values of VRM account for variability in both seafloor slope and aspect. This predictor describes the variation in terrain and should differentiate smooth and rugged substrates (Sappington et al., 2007; Grohmann et al., 2011). Finally, BPI is a measure of elevation relative to surrounding locations (Guisan et al., 1999). Values of BPI can be used to highlight topographic features, such as seafloor valleys or knolls, which are shallower or deeper than neighboring areas. Prior to our study, it was unclear whether the model that includes these 3 predictors, or seafloor characteristics, could be used to effectively classify seafloor trawlability outside of the study area utilized by Pirtle et al. (2015) or whether application of this model to other areas in the GOA would result in high misclassification.

The primary objective of our study was to use a combination of seafloor characteristics derived from multibeam sonar data and from analysis of underwater video images to determine whether the GLM that combines  $S_b$  oblique values with VRM and BPI values can continue to correctly classify seafloor trawlability over a larger extent of the GOA than the area classified by Pirtle et al. (2015). Secondly, we wanted to determine whether nonlinear models are better at predicting seafloor trawlability; therefore, we tested the effectiveness of 3 other

<sup>1</sup> Mention of trade names or commercial companies is for identification purposes only and does not imply endorsement by the National Marine Fisheries Service, NOAA.

model types (generalized additive models [GAMs], boosted regression trees [BRTs], and random forests [RFs]) in predicting seafloor trawlability in the GOA, using the same 3 seafloor characteristics used in the GLM. Finally, on the basis of the performances of the 4 models, we identified which of the 3 seafloor characteristics determined with multibeam sonar data are the most consistently useful to discriminate between trawlable and untrawlable seafloor.

## Materials and methods

### Field methods

Large-scale acoustic trawl surveys that assess the stock of walleye pollock (*Gadus chalcogrammus*) in the GOA are conducted biennially aboard the NOAA Ship *Oscar Dyson* during the summer (e.g., Jones et al.<sup>2,3,4</sup>). Fine-scale multibeam surveys were conducted with a Simrad ME70 opportunistically during the evening hours in 2011, 2013, and 2015. The multibeam surveys followed parallel transects spaced 2 km (1 nmi) apart, within nearby 25-km<sup>2</sup> grid cells. Only one fine-scale multibeam survey was conducted within each grid cell. Immediately after the multibeam survey, video data were also collected at 1–5 locations (i.e., camera stations) to characterize the extent of trawlable and untrawlable seafloor at areas covered during each fine-scale multibeam survey (Fig. 1). Selection of the locations of camera stations was often dependent on wind and current direction, sea state, and placement of other camera stations within the same grid. Fine-scale multibeam surveys were conducted in similar numbers of trawlable and untrawlable 25-km<sup>2</sup> grid cells. However, the extent of actual trawlable and untrawlable areas within a grid cell was unknown a priori, ultimately resulting in an unbalanced number of trawlable versus untrawlable camera stations.

**Multibeam surveys** The Simrad ME70 was configured with 31 symmetrical split beams, with the middle beam vertically oriented (i.e., steered at 0°). The beams in this configuration ranged from the spherical 2.8° nadir beam (0°) operating at 117 kHz to the 2 ellipsoidal 4.5°-along-ship-by-11.0°-athwartship beams steered from –66° to 66°

and operating at 75 kHz (Weber et al., 2013; Stienessen et al., 2019). A pulse duration of 1.5-ms was used for each beam. The sampling rate was synchronized with that of the ship's downward-looking Simrad EK60 scientific echo sounder (Kongsberg Maritime AS) to eliminate interference between the 2 instruments, resulting in an effective sampling interval of 1.35 s. A 25-mm tungsten carbide sphere was used to calibrate each beam by using the standard sphere calibration method (Demer et al.<sup>5</sup>).

A POS MV V4 system (Applanix, Richmond Hill, Canada) was used to compensate beam steering for pitch and roll of the vessel by exporting dynamic motion and position data directly into the Simrad ME70. It was also used to georeference the multibeam sonar data. A C-Nav MBX-4 system (Oceaneering International Inc., Houston, TX) was used to apply differential correction data to the POS MV to improve position accuracy. Expendable bathythermograph probes and casts of a conductivity, temperature, and depth instrument (SBE 911plus CTD, Sea-Bird Scientific, Bellevue, WA) were used to collect water temperature and salinity profile data at selected locations throughout the study area (Jones et al.<sup>2,3,4</sup>). Conductivity and water temperature data at transducer depth (5 m) were continuously transmitted to the Simrad ME70 sonar system from the ship's sensors.

**Camera stations** Camera stations were sampled during nighttime hours for all years, with one camera deployment conducted at each station. During camera deployments, the ship and camera were allowed to drift over the seafloor at a speed of approximately 1 kt (0.53 m/s). The depths of camera stations ranged between 75 and 300 m. A camera station is defined as the entire area over which a camera drifted during a particular deployment, and the location of a camera station is the location of the initial deployment. Selection of the locations of camera stations was often limited by current and wind speed and direction.

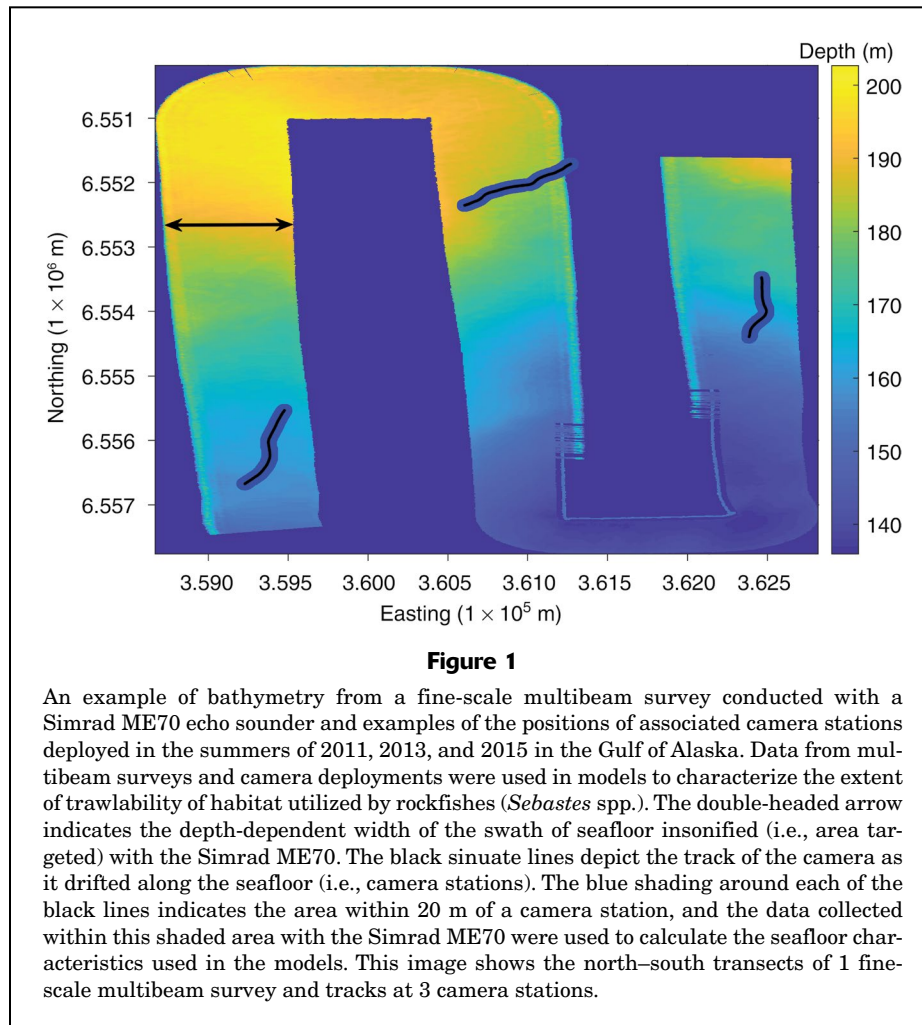
Video images were collected at camera stations by using either a single digital camera or a stereo digital camera (SDC) system in 2011 and by using only an SDC system in 2013 and 2015. The digital camera was equipped with one digital video recorder and 2 lights placed above the camera housing (Pirtle et al., 2015). The version of the SDC system used in 2011 had 2 Sony TRD-900 progressive scan camcorders (Sony Corp., Tokyo, Japan), both with a resolution of 1280 by 720 pixels, and 2 lights placed above the camera housing (Williams et al., 2010). Both video cameras resided in an aluminum cage. The version of the SDC system used in 2013 and 2015 is described in Rooper et al. (2016). It comprised paired machine-vision cameras that were spaced approximately 30 cm apart in underwater housing and were used to collect synchronized still images at a rate of 1 Hz. Lighting for this camera system was provided by 4 LED strobe lights. Each deployment of the

<sup>2</sup> Jones, D. T., P. H. Ressler, S. C. Stienessen, A. L. McCarthy, and K. A. Simonsen. 2014. Results of the acoustic-trawl survey of walleye pollock (*Gadus chalcogrammus*) in the Gulf of Alaska, June–August 2013 (DY2013-07). AFSC Process. Rep. 2014-16, 95 p. Alaska Fish. Sci. Cent., Natl. Mar. Fish. Serv., Seattle, WA. [Available from [website](#).]

<sup>3</sup> Jones, D. T., S. Stienessen, K. A. Simonsen, and M. A. Guttormsen. 2015. Results of the acoustic-trawl survey of walleye pollock (*Gadus chalcogrammus*) in the western/central Gulf of Alaska, June–August 2011 (DY2011-03). AFSC Process. Rep. 2015-04, 74 p. Alaska Fish. Sci. Cent., Natl. Mar. Fish. Serv., Seattle, WA. [Available from [website](#).]

<sup>4</sup> Jones, D. T., S. Stienessen, and N. Lauffenburger. 2017. Results of the acoustic-trawl survey of walleye pollock (*Gadus chalcogrammus*) in the Gulf of Alaska, June–August 2015 (DY2015-06). AFSC Process. Rep. 2017-03, 102 p. Alaska Fish. Sci. Cent., Natl. Mar. Fish. Serv., Seattle, WA. [Available from [website](#).]

<sup>5</sup> Demer, D. A., L. Berger, M. Bernasconi, E. Bethke, K. Boswell, D. Chu, R. Domokos, A. Dunford, S. Fässler, S. Gauthier, et al. 2015. Calibration of acoustic instruments. ICES Coop. Res. Rep. 326, 133 p. [Available from [website](#).]



single digital camera included 5 min on the seafloor, and each deployment of the SDC system included 15–30 min on the seafloor in 2011 or 30 min just above the seafloor in 2013 and 2015. The SDC system had a real-time video feed to the surface and a winch that allowed the camera position to be adjusted vertically in the water column as the camera drifted over rough terrain.

#### Data extraction and analysis

**Multibeam data** Bathymetry and backscatter data were extracted from the raw files retrieved from the Simrad ME70. More specifically, acoustic power associated with each detection of the seafloor was converted to backscatter following protocols established by Weber et al. (2013) in which system gains, calibration offsets, water column spherical spreading and absorption, and the area targeted by the beam are considered. Detections of the bottom were further used to calculate values for 3 seafloor characteristics identified by Pirtle et al. (2015) as among the best metrics with the best scale of analysis to predict seafloor trawlability in the GOA. The characteristics were

$S_b$  oblique, VRM, and BPI. The  $S_b$  oblique data were limited to the angle-dependent  $S_b$  data collected at incidence angles between 35° and 50°.

On the basis of results of Pirtle et al. (2015), VRM was calculated with data from a 21-by-21 array of 6-m<sup>2</sup> grid cells by using the bathymetry of each cell and 8 surrounding neighbor cells, and BPI was calculated with data from analysis windows, each with a radius of 200 6-m<sup>2</sup> grid cells. In our study, VRM was calculated by using only metric units (i.e., positions in meters of  $x$  and  $y$  coordinates in the Universal Transverse Mercator system and depth in centimeters). In contrast, Pirtle et al. (2015) used 2 different types of units for VRM calculations (i.e., positions in degrees of  $x$  and  $y$  coordinates in a geographic coordinate system and depth in meters).

Only seafloor characteristics calculated for the area within 20 m of a given camera station (i.e., within 20 m of the path of the camera as it drifted over the seafloor) were associated with that particular station. Specifically, if the bottom detection was within 20 m of the camera station, VRM and BPI were calculated, even if part or all of the array of 6-m<sup>2</sup> grid cells (VRM) or of the radius of the

analysis window (BPI) was outside of the 20 m. Single  $S_b$ , oblique, VRM, and BPI values were derived for each camera station by taking an average of each value collected along the camera path.

**Video data** Seafloor substrate was classified as either trawlable or untrawlable during review of video images by an experienced AFSC analyst. Designation of trawlability was based on whether the standard 4-seam Poly-Nor'Eastern bottom trawl used by AFSC in biennial bottom-trawl surveys (Stauffer, 2004) could successfully trawl in a given area. Specifically, analysts defined untrawlable areas in video images as any substrate containing boulders higher than 20 cm off bottom, an elevation that corresponds to the height of the roller gear on the footrope of the Poly-Nor'Eastern trawl (Rooper et al., 2012). They also classified areas in video images as untrawlable if the seafloor contained bedrock with vertical relief or ruggedness greater than 20 cm that would likely prevent the bottom trawl from passing over it without damage to the net from seafloor contact.

#### Modeling seafloor trawlability

Ultimately, each camera station was classified as either trawlable or untrawlable and was characterized by  $S_b$ , oblique, VRM, and BPI. The analyses done with models included only the stations for which data for all 3 variables were produced. Occasionally it was not possible to calculate  $S_b$ , oblique at a camera station. Although the camera deployment paths fell within the area covered during a fine-scale multibeam survey (Fig. 1), the positions of the camera deployments did not always overlap with the portion of the survey swath for which a Simrad ME70 collected data at 35–50° incidence angles. The effectiveness of using the seafloor characteristics derived from multibeam sonar data to discriminate between trawlable and untrawlable habitat was tested with 4 different kinds of predictive models: GLMs, GAMs, BRTs, and RFs. The GLMs were used to build upon, and allow direct comparisons to, the work of Pirtle et al. (2015). The GAMs are similar to the GLMs but allow any nonlinear relationships between the seafloor characteristics to be expressed. The BRTs and RFs have machine learning strength for classification and allow inclusion of nonlinear components.

**Generalized linear models** Seafloor trawlability was modeled with logistic regression by using the GLM:

$$\text{trawlability} = B_0 + (B_1 \times S_b \text{ oblique}) + (B_2 \times \text{VRM}) + (B_3 \times \text{BPI}) + E, \quad (1)$$

where  $B_{0,1,2,3}$  = the parameters estimated by the model, and

$E$  = error;

in the GLM, the logit link function  $p(Y)=e(Y)/1+e(Y)$  is used for binary response data (McCullagh and Nelder, 1983). The logit link function maps probability values ( $p$ ) between 0 and 1 for any given real number  $Y$  between

negative and positive infinity. Seafloor characteristics were standardized prior to analysis by subtracting the mean and dividing by the standard deviation.

We ran a GLM with all 3 years (2011, 2013, and 2015) of data. Backward variable selection was then performed on the data from all 3 years by fitting the model and dropping terms on the basis of an insignificant  $P$ -value for the model term (i.e.,  $P \geq 0.05$ ) and the Akaike information criterion (AIC). The predicted responses of models with AIC values within 2 digits are not considered different (Burnham and Anderson, 2002). Deviance explained ( $D^2$ ), an analysis of deviance test comparing the model results to a null model (level of significance=0.05), and the area under the receiver operating characteristic curve (AUC) were also calculated for comparison with the 3 other types of predictive models. In general, an AUC value of 0.5 indicates that the model cannot discriminate between trawlable and untrawlable seafloor; AUC values of 0.7–0.8 are acceptable, values of 0.8–0.9 are good, and values >0.9 are excellent (Hosmer and Lemeshow, 2000). To evaluate the performance of the GLMs, we fit a GLM to two-thirds of the data (randomly drawn without replacement) and used the remaining one-third of the data for testing. Closer agreement between the area under the receiver operating characteristic curve for the test data set containing out-of-sample data (test AUC) and the area under the receiver operating curve for the training data set (training AUC) indicates better predictive performance by the model.

**Generalized additive models** Seafloor trawlability was also modeled with GAMs by using the *mgecv* package, vers. 1.8-28 (Wood, 2017), in RStudio, vers. 1.2.5019-6 (RStudio, Boston, MA). These models assume that the effects of trawlability are additive and can use smooth functions (penalized regression splines) to model each predictor on the response variable (Wood and Augustin, 2002). Best-fitting models were determined in a backward stepwise fashion beginning with the GAM model:

$$\text{trawlability} = s(S_b \text{ oblique}) + s(\text{VRM}) + s(\text{BPI}) + E, \quad (2)$$

where the function  $s(x)$  indicates a smooth effect of each predictor. In the GAM, the logit link function is used for binary response data. Terms were dropped on the basis of a nonsignificant test for the  $F$ -term in the nonparametric effects, and terms were made into a linear function instead of a smooth function on the basis of a significant test for the  $F$ -term in the parametric effects. Model results were compared on the basis of values for  $D^2$ , AIC, and training AUC. To evaluate the performance of the GAMs, we fit a GAM to two-thirds of the data and used the remaining one-third of the data for testing (the same training and testing data sets used in the work with the GLMs).

**Boosted regression trees** Seafloor trawlability was modeled with BRTs by using the *dismo* package, vers. 1.1-4 (Hijmans et al., 2017), in RStudio. Unlike traditional regression tree methods, BRT boosting is used to combine large numbers of simple tree models adaptively to display

nonlinear relationships between the response and its predictors and to optimize predictive performance (e.g., Elith et al., 2006, 2008). That is, the input data are weighted in subsequent trees rather than allowing each occurrence to have an equal probability of being selected. Boosted regression trees require the specification of 3 parameters: learning rate, tree complexity (the number of nodes in the tree), and bag fraction (Elith et al., 2006, 2008). We ran the BRT model,

$$\text{trawlability} = S_b \text{ oblique} + \text{VRM} + \text{BPI}, \quad (3)$$

following the guidelines discussed in Elith et al. (2008) by using the Bernoulli family for binary response data and reducing the learning rate to aim for over 1000 trees. For example, we used a learning rate of 0.001 shrinkage applied per tree, a tree complexity of 5, and bag fraction of 0.5. We assessed the value in simplifying the model by using the `gbm.simplify` procedure in the `dismo` package. Two-thirds of the data were selected to be part of the training set, and the remaining one-third of the data were used as the test set (the same training and testing data sets used in the work with GLMs and GAMs). Model results were evaluated on the basis of values for  $D^2$ , AUC, and the influence of the predictors.

**Random forests** Seafloor trawlability was modeled with RFs by using the `randomForest` package, vers. 4.6-14 (Liaw and Wiener, 2002), and `caret` package, vers. 6.0-84 (Kuhn, 2019), in RStudio. In the RFs, random samples of predictor variables are used to generate many individual decision trees (forests) where each decision tree is constructed by an individual bootstrap with replacement sample drawn from the original data. That is, the split determination at each node is based on the best-splitting variable from a randomly selected subset of variables. For classification, a weighted vote of the decision trees is used (Breiman, 2001). Data not in the bootstrap sample are out-of-bag data and are used as samples to be classified in each decision tree. Random forests require the specification of 2 parameters: number of classification trees (number of bootstrap iterations) and the number of input variables to be used at each node. An RF has reliable predictive performance even when most predictive variables are noisy; therefore, it does not require preselection of predictors (Díaz-Uriarte and Alvarez de Andres, 2006; Okun and Priisalu, 2007).

On the basis of the results of a sensitivity analysis, we found that the `caret` package defaults (number of trees set at 500, and number of input variables set at 1) are appropriate for our data and used them in the RF model:

$$\text{trawlability} = S_b \text{ oblique} + \text{VRM} + \text{BPI}. \quad (4)$$

Two-thirds of the data were selected to be part of the training set, and the remaining one-third of the data were used as the test set (the same training and testing data sets used in the work with the GLMs, GAMs, and BRTs). Model results were evaluated on the basis of values for the out-of-bag error estimate, AUC, and mean decrease in the accuracy of the predictors.

**Ensemble model** An ensemble model was produced for estimation of seafloor trawlability by averaging predictions of the best GLM, GAM, BRT, and RF at each raster cell (i.e., for each camera station). Two-thirds of the data were selected to be part of the training set, and the remaining one-third of the data were used as the test set (the same training and testing data sets used in the GLM, GAM, BRT, and RF) to compare the ensemble model fit to the individual models.

## Results

A total of 47, 64, and 92 camera stations were sampled during the fine-scale surveys conducted with a Simrad ME70 during 2011, 2013, and 2015, respectively. Of these, only 38 (21 trawlable and 17 untrawlable) camera stations in 2011, 36 (22 trawlable and 14 untrawlable) camera stations in 2013, and 56 (29 trawlable and 27 untrawlable) camera stations in 2015 produced data that could be used to estimate all 3 seafloor characteristics (Fig. 2). This was largely due to the fact that the video data were collected outside of the portion of the swath surveyed with a Simrad ME70 that was characterized by 35–50° incidence angles (i.e., there were no overlapping measures for  $S_b$  oblique) at a number of camera stations. This effect, coupled with the unknown extent of trawlable and untrawlable areas within a grid cell a priori, produced an unbalanced final number of trawlable and untrawlable camera stations.

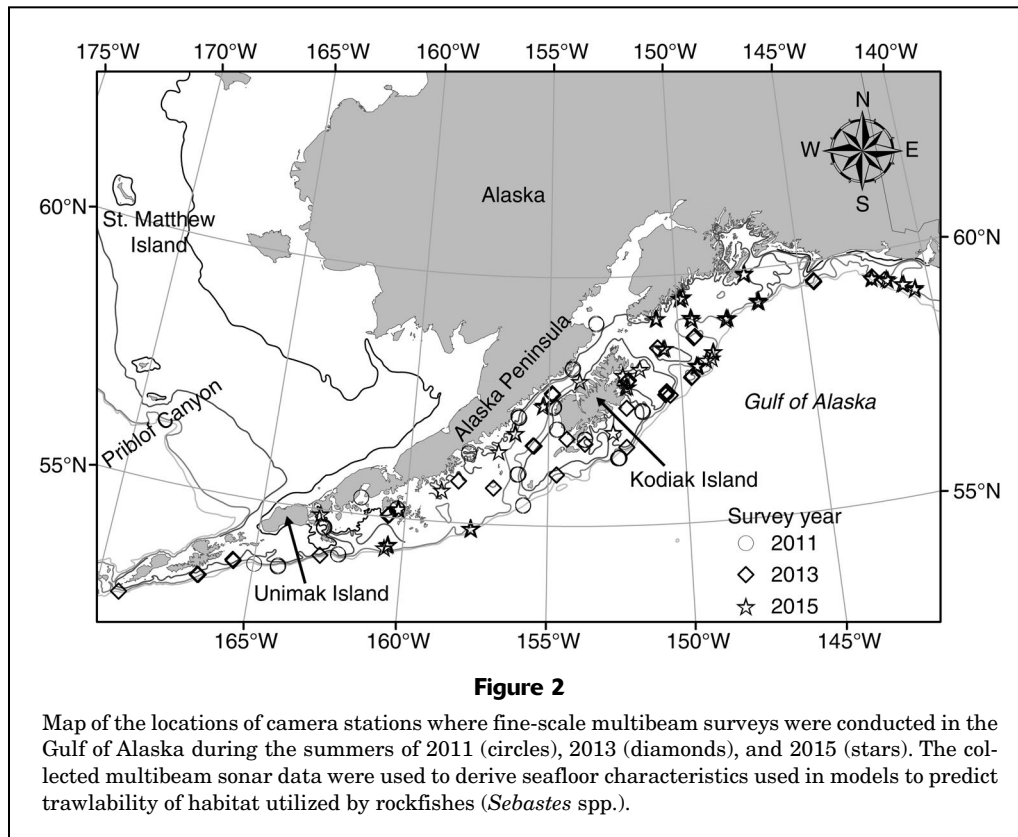
The seafloor characteristic  $S_b$  oblique had a low correlation with the other 2 characteristics (VRM: coefficient of correlation  $|r|=0.15$ ; BPI:  $r=0.05$ ), and VRM and BPI also had a low correlation with one another ( $r=0.09$ ). Values of  $S_b$  oblique associated with trawlable seafloor were significantly lower than those associated with untrawlable seafloor when all 3 years of data were used (Fig. 3A). Values of VRM and BPI associated with trawlable seafloor were also lower than those associated with untrawlable seafloor when all 3 years of data were used, although the differences were not significant (Fig. 3, B and C).

### Generalized linear model

The best-fit GLM was a single-variable model in which  $S_b$  oblique is used. Only  $S_b$  oblique was significant in the full model ( $P=0.0001$ ). The variables VRM ( $P=0.11$ ) and BPI ( $P=0.22$ ) were not. Additionally, the AIC value for the single-variable model in which only  $S_b$  oblique (AIC=151.5) is used was slightly less than that for the full model (AIC=153.4) (Table 1).

### Generalized additive model

The best-fit GAM included a smoothed VRM term and a linearized  $S_b$  oblique term. The BPI seafloor characteristic was not significant for the model. In the best model, the remaining terms were significant, linearized  $S_b$  oblique was significant, AIC (147.5) was minimized, and  $D^2$  (0.31) was relatively high (Table 2). Compared with this model, a



model that included a smooth function for  $S_b$  oblique had a higher AIC (150.5), although the  $D^2$  (0.31) was the same. A model that included all 3 seafloor characteristics and assigned a smooth function to them had an even higher AIC (154.4), and the  $D^2$  (0.25) was lower.

#### Boosted regression tree

Results from the use of the `gbm.simplify` procedure indicate that the full BRT model (with all 3 variables) could be simplified to a 2-variable model by dropping VRM. This simplification resulted in a more parsimonious model without degradation of model fit. That is, the removal of VRM did not adversely affect model predictive performance. Deviance explained (0.31) was the same for the 2 models, and test AUC increased by 0.01 (to 0.65) in the simplified model. The predictor  $S_b$  oblique influenced both models the most (68% in the simplified model and 59% in the full model), followed by BPI (simplified: 32%; full: 28%). The VRM influenced the full model by only 13% (Table 3).

#### Random forest

The global accuracy (proportion of correct classification of trawlability) for this model was 0.655. Restated, the RF incorrectly classified trawlability 34.5% of the time (out-of-bag error estimate=0.345). The seafloor characteristic

$S_b$  oblique contributed the most to the model's prediction performance (mean decrease accuracy=0.180), but permuting VRM (mean decrease accuracy=0.013) and BPI (mean decrease accuracy=0.006) did not obstruct the model substantially. That is, VRM and BPI were not helpful predictors. When either VRM or BPI was permuted in a way that allowed its distribution to remain the same but assigned its specific observations randomly to the data, there was minimal loss of accuracy in classification.

#### Model evaluation

Results from all full models indicate a strong relationship between seafloor trawlability and  $S_b$  oblique. Additionally,  $S_b$  oblique was the most important predictor in all models. The seafloor characteristic VRM was significant in the GAM, and BPI contributed to the performance of the BRT. The GLM and GAM produced smooth or linear responses, but the significance of VRM was not consistent in these 2 models (Fig. 4). The response curves for the BRT and RF were similar to each other, indicating that the use of these 2 models revealed the same relationships in the data (Fig. 4), although the different learning methods between the 2 models resulted in different associations. In the RF, the initial variable is selected at random, and over many iterations the choice typically becomes obvious (e.g.,  $S_b$  oblique). However, when similar predictions result from

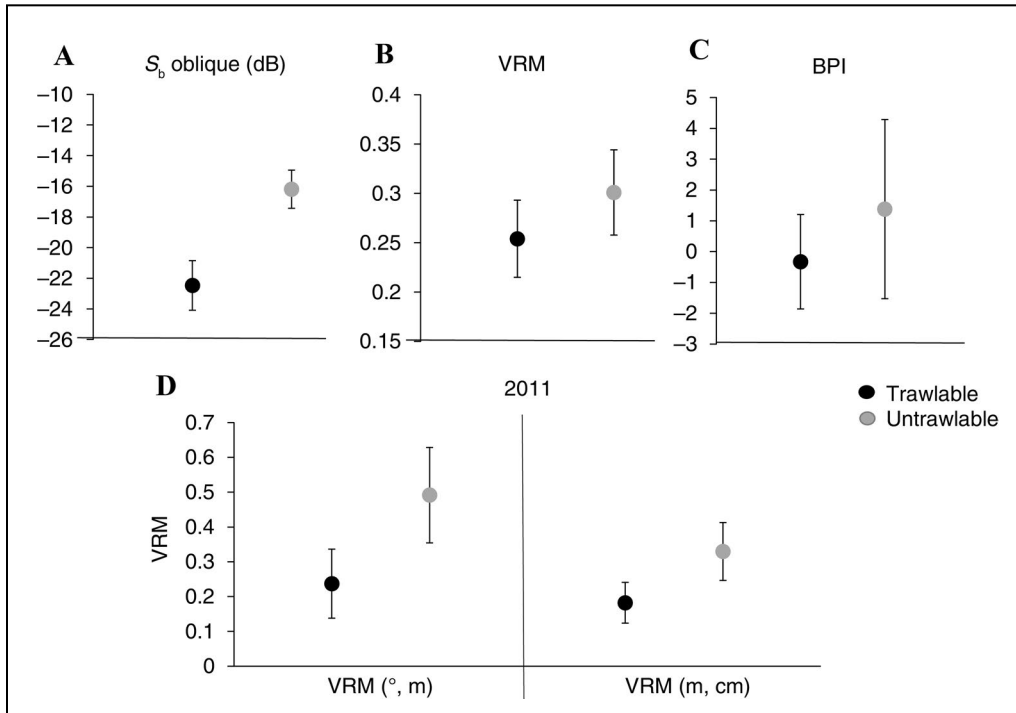


**Figure 3**

Mean values of seafloor characteristics derived from multibeam sonar data and used in models to classify habitat utilized by rockfishes (*Sebastes* spp.) as trawlable (black circles) or untrawlable (gray circles). Data were collected during fine-scale multibeam surveys conducted in 2011, 2013, and 2015 in the Gulf of Alaska. Plots show the effect of trawlability on 3 seafloor characteristics, (A) oblique incidence backscatter strength ( $S_b$  oblique), (B) vector ruggedness measure (VRM), and (C) bathymetric position index (BPI), over all years combined and (D) show the effect of units on VRM in 2011. In this study, VRM was calculated by using meters for coordinates in the Universal Transverse Mercator system and depth in centimeters (right half of the plot in panel D), but Pirtle et al. (2015) used degrees for coordinates in a geographic coordinate system and depth in meters (left half of the plot). Error bars indicate 95% confidence intervals.

**Table 1**

Comparison of results from generalized linear models used to predict seafloor trawlability of habitat utilized by rockfishes (*Sebastes* spp.) at locations of camera stations surveyed during 2011, 2013, and 2015 in the Gulf of Alaska. Predictor variables are seafloor characteristics derived from multibeam sonar data: oblique incidence backscatter strength ( $S_b$  oblique), vector ruggedness measure (VRM), and bathymetric position index (BPI). Values of Akaike information criterion (AIC), deviance explained ( $D^2$ ), area under the receiver operating curve for the training data set (training AUC), and area under the receiver operating curve for the test data set containing out-of-sample data (test AUC) are provided for each model.

Year range	Model	AIC	$D^2$	Model significance	Training AUC	Test AUC
2011–2015	$S_b$ oblique	151.5	0.17	$2.34 \times 10^{-8}$	0.77	0.75
2011–2015	$S_b$ oblique + VRM + BPI	153.4	0.19	$2.78 \times 10^{-7}$	0.81	0.73

models with 2 different variables (e.g., models with VRM or BPI), the randomness of the RF becomes more apparent.

Model fits were reasonable for each best model (test AUC values range from 0.63 to 0.75), with the best GLM

and GAM having higher test AUC scores (0.75 and 0.70, respectively) than the simplified BRT model and RF (0.65 and 0.63, respectively) (Tables 1–3). However, both the best GAM and simplified BRT accounted for more  $D^2$  (0.31; Tables 2–3) than the best GLM (0.17; Table 1).

## Ensemble model

The ensemble model was produced by averaging the predictions of the best models (i.e., the single-variable GLM in which  $S_b$  oblique was used, the GAM that included a smoothed VRM term and a linearized  $S_b$  oblique term, the simplified BRT, and the full RF) for each camera station. The fit for the ensemble model indicates that the model was reasonably effective in separating trawlable and untrawlable habitat (test AUC=0.70). The ensemble model's performance in predicting trawlability with the test data was better than the performance of the simple BRT (AUC=0.65; Table 3) and RF (AUC=0.63), it was equal to

the performance of the best GAM (AUC=0.70; Table 2), and it was slightly lower than the performance of the best GLM (AUC=0.75; Table 1).

## Discussion

All 4 types of predictive models produced similar overall results:  $S_b$  oblique was the most significant predictor to discriminate between seafloor designated as trawlable or untrawlable through analysis of video images, and all tested models were moderately effective in predicting trawlability at camera stations across the shelf in the GOA ( $D^2$  range from 0.17 to 0.31, and test AUC values range from 0.63 to 0.73). Results from the GAM and BRT indicate that one predictor can be omitted, but they disagree as to whether the predictor should be BPI (GAM) or VRM (BRT). Results from the GLM and RF indicate that both BPI and VRM could be omitted without much loss in the accuracy of the classification of trawlable versus untrawlable habitat.

The prominence of  $S_b$  oblique in predicting trawlability corroborates the results of previous work (Jagiello et al., 2003), specifically those studies on trawlability in the GOA (Weber et al., 2013; Pirtle et al., 2015), but over a much larger geographic extent. Additionally, the lower values of  $S_b$  oblique associated with trawlable areas compared with those associated with untrawlable areas indicate a lack of strong scatterers, like hard rock and boulders, in trawlable habitat (Jackson and Richardson, 2007; Lamarche et al., 2011). Weber et al. (2013) found that trawlable areas had lower  $S_b$  oblique values than untrawlable areas at Snakehead Bank in the GOA. Furthermore, of the measured seafloor characteristics,  $S_b$  oblique had the best performance in predicting trawlability at the Snakehead Bank study site (Weber et al., 2013). Pirtle et al. (2015) also found that untrawlable areas had higher  $S_b$  oblique values than trawlable areas at many locations between Akutan Island (53°43'N, 164°58'W) and the eastern side of Kodiak Island (57°18'W, 151°30'N). In their

**Table 2**

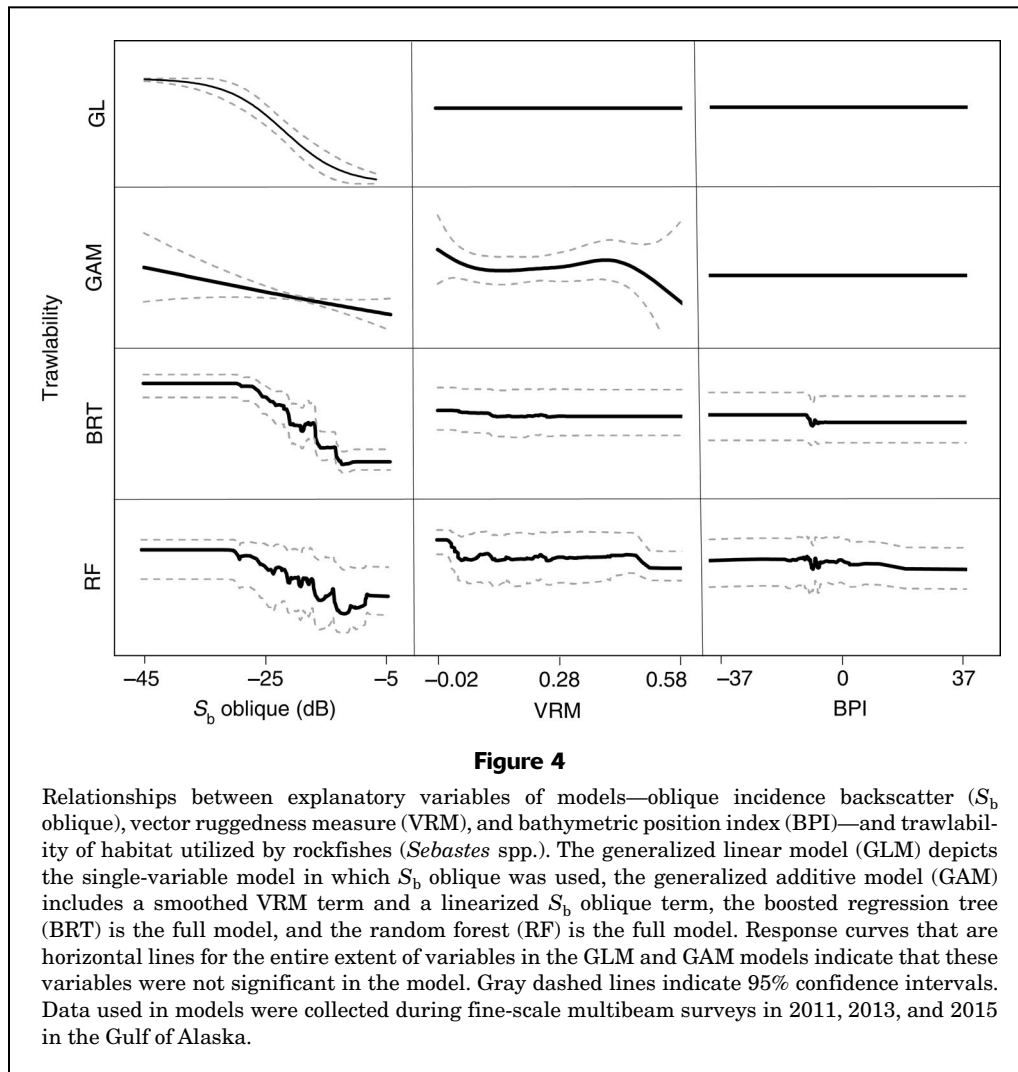
Comparison of results from generalized additive models used to predict seafloor trawlability of habitat utilized by rockfishes (*Sebastes* spp.) at locations of camera stations surveyed during 2011, 2013, and 2015 in the Gulf of Alaska. In the models,  $s(x)$  indicates a smooth effect of the predictor. Models are listed in order of decreasing accuracy of the predictions of trawlability. Predictor variables are seafloor characteristics derived from multibeam sonar data: oblique incidence backscatter strength ( $S_b$  oblique), vector ruggedness measure (VRM), and bathymetric position index (BPI). Values of Akaike information criterion (AIC), deviance explained ( $D^2$ ), area under the receiver operating curve for the training data set (training AUC), and area under the receiver operating curve for the test data set containing out-of-sample data (test AUC) are provided for each model.

Model	AIC	$D^2$	Training AUC	Test AUC
$S_b$ oblique + $s$ (VRM)	147.5	0.31	0.86	0.70
$s(S_b$ oblique) + $s$ (VRM)	150.5	0.31	0.87	0.70
$s(S_b$ oblique) + $s$ (VRM) + $s$ (BPI)	154.4	0.25	0.88	0.68

**Table 3**

Comparison of results from boosted regression trees, with 2 or 3 variables, used to predict seafloor trawlability of habitat utilized by rockfishes (*Sebastes* spp.) at locations of camera stations surveyed during 2011, 2013, and 2015 in the Gulf of Alaska. Predictor variables are seafloor characteristics derived from multibeam sonar data: oblique incidence backscatter strength ( $S_b$  oblique), vector ruggedness measure (VRM), and bathymetric position index (BPI). Values of deviance explained ( $D^2$ ), area under the receiver operating curve for the training data set (training AUC), and area under the receiver operating curve for the test data set containing out-of-sample data (test AUC) are provided for each model. The dash in the table signifies that the corresponding predictor variable (VRM) was not used in the associated model.

Model	$D^2$	$S_b$ oblique influence	VRM influence	BPI influence	Training AUC	Test AUC
$S_b$ oblique + BPI	0.31	68.2	–	31.8	0.86	0.65
$S_b$ oblique + VRM + BPI	0.31	59.3	13.1	27.6	0.88	0.64



study, characteristics derived from multibeam sonar data were used to predict seafloor trawlability for both locations of camera stations and for historic locations of trawl tows of the AFSC bottom-trawl survey. The latter was defined as areas where a bottom-trawl survey had previously been conducted, either successfully with little or no gear damage (trawlable) or unsuccessfully with extensive gear damage (untrawlable). For both camera station and trawl tow locations, Pirtle et al. (2015) found that a model in which only  $S_b$  oblique is used to be among the most discriminating single-variable models for predicting trawlability. Furthermore, the addition of other variables did not improve predictive discrimination for data from tow locations.

The relevance of VRM and BPI in predicting trawlability is less clear. Results of our study indicate that the addition of VRM and BPI does not improve on the effectiveness of a single-variable linear model in which only  $S_b$  oblique is used to predict trawlability. Similarly, in other studies, seafloor rugosity was a poor discriminator between trawlable and untrawlable seafloor at Snakehead Bank (Weber et al., 2013), and neither VRM nor BPI

improved on the performance of the single-variable linear model in predicting trawlability at tow locations over larger portions of the GOA (Pirtle et al., 2015). However, the addition of both VRM and BPI improved the effectiveness of the single-variable linear model in predicting trawlability at camera stations in the study of Pirtle et al. (2015). They found that including  $S_b$  oblique, VRM, and BPI resulted in 1 of the 2 most discriminating GLMs for explaining trawlability in the GOA ( $AIC=32.1$ ,  $D^2=0.55$ ). They calculated VRM slightly differently than we did, but that difference does not appear to explain the discrepancy in results. When we updated the data from 2011 used in the Pirtle et al. (2015) study with VRM calculated with consistent units (i.e., updated with positions in meters of  $x$  and  $y$  coordinates in the Universal Transverse Mercator system and depth in centimeters), the relationship between trawlable and untrawlable areas determined by using VRM values did not change. The VRM values for trawlable areas were still significantly lower than values for untrawlable areas (Fig. 3D), although the performance of the model decreased slightly ( $AIC=33.4$ ,  $D^2=0.45$ ).

When 2 more years of data (i.e., data from 2013 and 2015) were added to the model, performance decreased further (AIC=153.4;  $D^2=0.19$ ; Table 1).

Pirtle et al. (2015) postulated that VRM and BPI were important in predicting trawlability at locations of camera stations but not at trawl tow locations because at camera stations the range of seafloor types that was sampled (i.e., both trawlable and untrawlable) was broader than the range sampled at tow locations where surveys were designed to target trawlable seafloor. However, with the addition of the data from 2013 and 2015 to the linear model that incorporates a broader range of seafloor types, VRM and BPI were no longer necessary predictors. The portions of the GOA where data were collected from camera stations were larger in 2013 and 2015 than in 2011 (Fig. 1). That is, they were collected farther west (i.e., west of Umnak Island:  $52^{\circ}38'N$ ,  $169^{\circ}14'W$ ) and farther east (i.e., east of Kodiak Island) (Fig. 2). This difference indicates that VRM and BPI are not as effective in GLM predictive discrimination of trawlability beyond the geographic area sampled in 2011.

The power of the use of seafloor characteristics derived from multibeam sonar data to predict seafloor structures is dependent on spatial scale (Wilson et al., 2007). That is, the predictive power of the seafloor characteristics is dependent on the areal extent used to initially create the model. The predictive power of the characteristics is also

more pronounced when they have a greater range of values. The ranges of BPI values extracted in 2013 and 2015 were not as large as the range of those extracted in 2011 (Fig. 5). The VRM and BPI may be more useful as predictors when more “extreme” bottom types are encountered, and they may not have as much predictive power when their extracted values are closer to the overall mean. The areal extent of the study site used by Pirtle et al. (2015) to create the model likely affects the applicability of the model over a larger extent of the GOA.

Even though VRM and BPI can be omitted from the GLMs and RFs without much loss in effectiveness at defining trawlable versus untrawlable seafloor in the GOA, they were independently useful for predictive discrimination of trawlability in the GAMs and BRTs. That is, VRM was included in the most parsimonious GAM, and BPI was included in the most parsimonious (i.e., simplified) BRT. It is unclear why predictive performance with VRM and BPI is not consistent among the GAMs and BRTs, because these characteristics are not strongly correlated. They measure different seafloor properties; therefore, there should be no confusion about which characteristic should be dropped from the model. The addition of either VRM or BPI to the respective nonlinear models results in reasonable test AUC scores for the out-of-sample sites.

Our results indicate that all the models identify  $S_b$  oblique as the primary driver for predictive discrimination

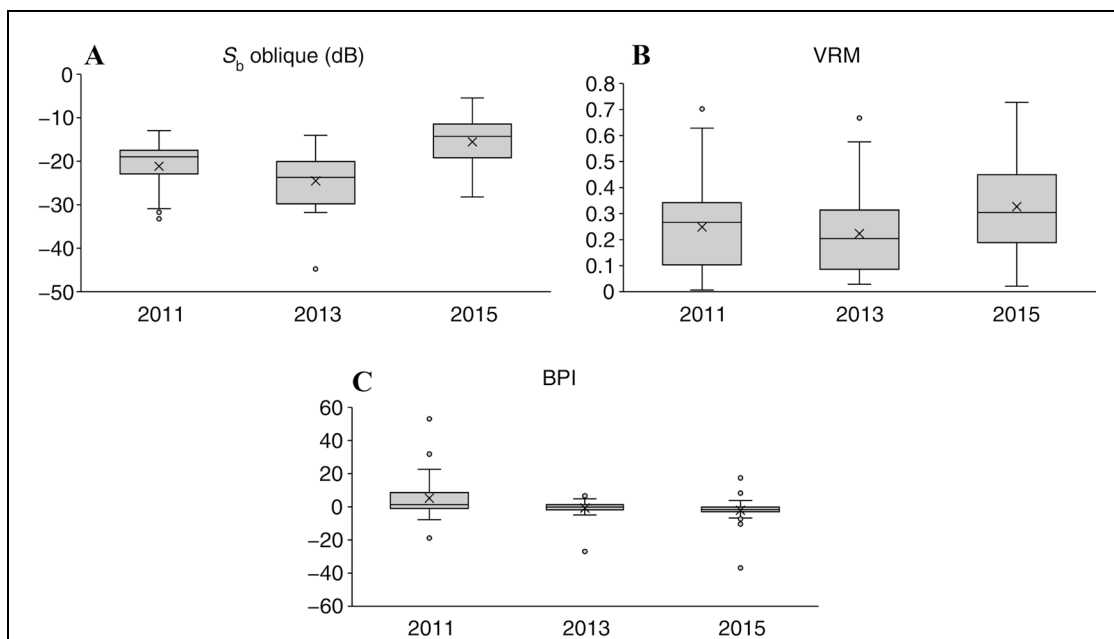


**Figure 5**

Box plots for the seafloor characteristics, (A) oblique incidence backscatter ( $S_b$  oblique), (B) vector ruggedness measure (VRM), and (C) bathymetric position index (BPI), derived from data collected with a Simrad ME70 multibeam echo sounder in 2011, 2013, and 2015 in the Gulf of Alaska. Seafloor characteristics were used to predict trawlability of habitat utilized by rockfishes (*Sebastes* spp.). The boxes show the first quartile (lower line), median (middle line), and third quartile (upper line). The whiskers extend to the minimum and maximum values. Gray circles represent outliers, and the x in the middle of each box indicates the mean.

of seafloor trawlability. This finding may encourage steering a scientific echo sounder's single beam between 35° and 50° to collect the necessary data. Single-beam echo sounders are fairly ubiquitous on both scientific and fishing vessels. Research results indicate that, when added to models that help explain distribution of benthic animals relative to their habitat, data collected with echo sounders increase the percentage of explained variance (McConnaughey and Syrjala, 2009; Somerton et al., 2017). However,  $S_b$  oblique is an incidence angle measurement, and is not dependent on steering angle. Theoretically, steering a single-beam echo sounder at 35–50° over flat terrain would yield the appropriate incidence angles. Yet as soon as there was any change in seafloor bathymetry, the incidence angles would also change, likely outside of the range of the steered single beam. Therefore, multibeam echo sounders are well-suited to collecting  $S_b$  oblique data. Having beams steered at a range of angles (from –66° to 66° in our study) increases the odds that at any given time one or more of the beams will insonify the seafloor at angles between 35° and 50°.

A limitation to using seafloor characteristics derived from multibeam sonar data to predict trawlability is that such data are restricted to the area within the width of the swath of the sonar and not necessarily applicable to the area outside of the swath. Additionally, seafloor characteristics cannot be calculated near the boundary of the swath, because of the prerequisite spatial scale of the analysis window needed to calculate them. The effect of this limitation is less for multibeam surveys with 100% bottom coverage (Pirtle et al., 2015). However, the “effective area” for extracting data on seafloor characteristics is further reduced by the inclusion of  $S_b$  oblique. This predictor can be derived from only small areas of the sonar swath (i.e., incidence angles of 35–50°), effectively prohibiting full bottom coverage. That is, data collected at incidence angles <35° and >50° are not useful in predicting seafloor trawlability.

## Conclusions

The GLM that combines  $S_b$  oblique values with VRM and BPI values produces reliable classification (on the basis of AUC results) of seafloor trawlability, even when applied to a larger geographic extent than that in previous work on seafloor trawlability in the GOA (Weber et al., 2013; Pirtle et al., 2015). However, VRM and BPI are not always critical predictors to the GLM—they are only beneficial in specific areas within the GOA (e.g., over the extent of the area sampled by Pirtle et al., 2015). The nonlinear models are not better at predicting seafloor trawlability, but the inclusion of VRM or BPI is more beneficial to these models and requires minimal computation effort.

These results indicate that, to predict seafloor trawlability in the GOA, it is important to use a model that has been developed with data from the entire extent of the area to which the model is being applied. Although results indicate that  $S_b$  oblique is a robust predictor of trawlability over both small and large extents of the GOA,

the usefulness of the other seafloor characteristics may be limited to specific areas of the GOA. Consequentially, the use of seafloor characteristics derived from multibeam sonar data in models to predict seafloor trawlability is essential because the models are dependent on spatial representation across the specific area of interest within the GOA.

The strength of the case for using models, rather than analysis of video images from camera deployments, to predict seafloor trawlability is the fact that multibeam sonar data can be collected relatively quickly and efficiently. A camera deployment on bottom for 30 min collects data only over an area that is approximately 1 m wide and 0.9 km long on the seafloor, whereas the Simrad ME70 echo sounder collects multibeam data across a swath width of 335–1345 m (which corresponds to the range of camera stations at depths between 75–300 m) and along a track of 10.2 km (assuming the ship is moving at 11 kt) during the same time period (i.e., 30 min). Reliable estimates of the extent of trawlable and untrawlable seafloor can be used to improve the accuracy of acoustic backscatter attributed to rockfishes in grid cells for areas classified as untrawlable (Jones et al., 2021), in turn improving the accuracy of stock assessments for these species.

## Acknowledgments

We thank the scientists and crew of the NOAA Ship *Oscar Dyson* for their hard work in helping with the data collection. We thank T. Honkalehto and C. O'Leary for valuable comments and remarks on earlier drafts of this paper.

## Literature cited

- Aydin, K., S. Barbeaux, M. Bryan, S. Cleaver, C. Cunningham, O. Davis, M. Dorn, A. Dreary, K. Echave, C. Faunce, et al. 2019. Stock assessment and fishery evaluation report for the groundfish resources of the Gulf of Alaska, 43 p. North Pac. Fish. Manage. Council, Anchorage, AK. [Available from [website](#).]
- Breiman, L. 2001. Random forests. *Mach. Learn.* 45:5–32. [Crossref](#)
- Brown, C. J., and P. Blondel. 2009. Developments in the application of multibeam sonar backscatter for seafloor habitat mapping. *Appl. Acoust.* 70:1242–1247. [Crossref](#)
- Burnham, K. P., and D. R. Anderson. 2002. Model selection and multi-model inference: a practical information-theoretic approach, 2nd ed., 488 p. Springer, New York.
- Cordue, P. L. 2007. A note on non-random error structure in trawl survey abundance indices. *ICES J. Mar. Sci.* 64:1333–1337. [Crossref](#)
- Cutter, G. R., Jr., L. Berger, and D. A. Demer. 2010. A comparison of bathymetry mapped with the Simrad ME70 multibeam echosounder operated in bathymetric and fisheries modes. *ICES J. Mar. Sci.* 67:1301–1309. [Crossref](#)
- Díaz-Urriarte, R., and S. Alvarez de Andrés. 2006. Gene selection and classification of microarray data using random forest. *BMC Bioinf.* 7:3. [Crossref](#)

- Elith, J., C. H. Graham, R. P. Anderson, M. Dudík, S. Ferrier, A. Guisan, R. J. Hijmans, F. Huettmann, J. R. Leathwick, A. Lehmann, et al.  
2006. Novel methods improve prediction of species' distributions from occurrence data. *Ecography* 29:129–151. [Crossref](#)
- Elith, J., J. R. Leathwick, and T. Hastie.  
2008. A working guide to boosted regression trees. *J. Anim. Ecol.* 77:802–813. [Crossref](#)
- Goff, J. A., B. J. Kraft, L. A. Mayer, S. G. Schock, C. K. Sommerfield, H. C. Olsen, S. P. S. Gulick, and S. Nordfjord.  
2004. Seabed characterization on the New Jersey middle and outer shelf: correlatability and spatial variability of seafloor sediment properties. *Mar. Geol.* 209:147–172. [Crossref](#)
- Grohmann, C. H., M. J. Smith, and C. Riccomini.  
2011. Multiscale analysis of topographic surface roughness in the midland valley, Scotland. *IEEE Trans. Geosci. Remote Sens.* 49:1200–1213. [Crossref](#)
- Guisan, A., S. B. Weiss, and A. D. Weiss.  
1999. GLM versus CCA spatial modeling of plant species distribution. *Plant Ecol.* 143:107–122. [Crossref](#)
- Hijmans, R. J., S. Phillips, J. Leathwick, and J. Elith.  
2017. dismo: species distribution modeling. R package, vers. 1.1-4. [Available from [website](#), accessed October 2019.]
- Hosmer, D. W., and S. Lemeshow.  
2000. *Applied logistic regression*, 2nd ed., 392 p. John Wiley and Sons, New York.
- Jackson, D. R., and M. D. Richardson.  
2007. *High-frequency seafloor acoustics*, 616 p. Springer, New York.
- Jagiello, T., A. Hoffmann, J. Tagart, and M. Zimmermann.  
2003. Demersal groundfish densities in trawlable and untrawlable habitats off Washington: implications for the estimation of habitat bias in trawl surveys. *Fish. Bull.* 101:545–565.
- Jones, D. T., C. D. Wilson, A. De Robertis, C. N. Rooper, T. C. Weber, and J. L. Butler.  
2012. Evaluation of rockfish abundance in untrawlable habitat: combining acoustic and complementary sampling tools. *Fish. Bull.* 110:332–343.
- Jones, D. T., C. N. Rooper, C. D. Wilson, P. D. Spencer, D. H. Hanselman, and R. E. Wilborn.  
2021. Estimates of availability and catchability for select rockfish species based on acoustic-optic surveys in the Gulf of Alaska. *Fish. Res.* 236:105848. [Crossref](#)
- Kuhn, M.  
2019. caret: classification and regression training. R package, vers. 6.0-84. [Available from [website](#), accessed January 2020.]
- Lamarque, G., X. Lurton, A.-L. Verdier, and J.-M. Augustin.  
2011. Quantitative characterisation of seafloor substrate and bedforms using advanced processing of multibeam backscatter—application to Cook Strait, New Zealand. *Cont. Shelf Res.* 31(Suppl. 2):S93–S109. [Crossref](#)
- Liaw, A., and M. Wiener.  
2002. Classification and regression by randomForest. *R News* 2(3):18–22.
- McConnaughey, R. A., and S. E. Syrjala.  
2009. Statistical relationships between the distributions of groundfish and crabs in the eastern Bering Sea and processed returns from a single-beam echosounder. *ICES J. Mar. Sci.* 66:1425–1432. [Crossref](#)
- McCullagh, P., and J. A. Nelder.  
1983. *Generalized linear models*, 261 p. Chapman and Hall, New York.
- Okun, O., and H. Priisalu.  
2007. Random forest for gene expression based cancer classification: overlooked issues. In *Pattern recognition and image analysis. IbPRIA 2007. Lecture notes in computer science*, vol. 4478 (J. Martí, J. M. Benedí, A. M. Mendonça, and J. Serrat, eds.), p. 438–490. Springer, Berlin, Germany.
- Pirtle, J. L., T. C. Weber, C. D. Wilson, and C. N. Rooper.  
2015. Assessment of trawlable and untrawlable seafloor using multibeam-derived metrics. *Methods Oceanogr.* 12:18–35. [Crossref](#)
- Rooper, C. N., M. H. Martin, J. L. Butler, D. T. Jones, and M. Zimmermann.  
2012. Estimating species and size composition of rockfishes to verify targets in acoustic surveys of untrawlable areas. *Fish. Bull.* 110:317–331.
- Rooper, C. N., M. F. Sigler, P. Goddard, P. Malecha, R. Towler, K. Williams, R. Wilborn, and M. Zimmerman.  
2016. Validation and improvement of species distribution models for structure-forming invertebrates in the eastern Bering Sea with an independent survey. *Mar. Ecol. Prog. Ser.* 551:117–130. [Crossref](#)
- Sappington, J. M., K. M. Longshore, and D. B. Thompson.  
2007. Quantifying landscape ruggedness for animal habitat analysis: a case study using bighorn sheep in the Mojave Desert. *J. Wildl. Manage.* 71:1419–1426. [Crossref](#)
- Somerton, D. A., R. A. McConnaughey, and S. S. Intelmann.  
2017. Evaluating the use of acoustic bottom typing to inform models of bottom trawl sampling efficiency. *Fish. Res.* 185:14–16. [Crossref](#)
- Stauffer, G.  
2004. NOAA protocols for groundfish bottom trawl surveys of the nation's fishery resources. NOAA Tech. Memo. NMFS-F/SPO-65, 205 p.
- Stienessen, S. C., C. D. Wilson, T. C. Weber, and J. K. Parrish.  
2019. External and internal grouping characteristics of juvenile walleye pollock in the eastern Bering Sea. *Aquat. Living Resour.* 32:19. [Crossref](#)
- Trenkel, V. M., V. Mazauric, and L. Berger.  
2008. The new fisheries multibeam echosounder ME70: description and expected contribution to fisheries research. *ICES J. Mar. Sci.* 65:645–655. [Crossref](#)
- von Szalay, P. G., and N. W. Raring.  
2018. Data report: 2017 Gulf of Alaska bottom trawl survey. NOAA Tech. Memo. NMFS-AFSC-374, 260 p.
- Weber, T. C., C. Rooper, J. Butler, D. Jones, and C. Wilson.  
2013. Seabed classification for trawlability determined with a multibeam echo sounder on Snakehead Bank in the Gulf of Alaska. *Fish. Bull.* 111:68–77. [Crossref](#)
- Williams, K., C. N. Rooper, and R. Towler.  
2010. Use of stereo camera systems for assessment of rockfish abundance in untrawlable areas and for recording pollock behavior during midwater trawls. *Fish. Bull.* 108:352–362.
- Wilson, M. F. J., B. O'Connell, C. Brown, J. C. Guinan, and A. J. Grehan.  
2007. Multiscale terrain analysis of multibeam bathymetry data for habitat mapping on the continental slope. *Mar. Geod.* 30:3–35. [Crossref](#)
- Wood, S. N.  
2017. *Generalized additive models: an introduction with R*, 2nd ed., 496 p. CRC Press, Boca Raton, FL.
- Wood, S. N., and N. H. Augustin.  
2002. GAMs with integrated model selection using penalized regression splines and applications to environmental modelling. *Ecol. Model.* 157:157–177. [Crossref](#)